

# Electrocoagulation of colloidal biogenic selenium

Lucian C. Staicu · Eric D. van Hullebusch ·  
Piet N. L. Lens · Elizabeth A. H. Pilon-Smits ·  
Mehmet A. Oturan

Received: 18 July 2014 / Accepted: 9 September 2014 / Published online: 20 September 2014  
© Springer-Verlag Berlin Heidelberg 2014

**Abstract** Colloidal elemental selenium (Se(0)) adversely affects membrane separation processes and aquatic ecosystems. As a solution to this problem, we investigated for the first time the removal potential of Se(0) by electrocoagulation process. Colloidal Se(0) was produced by a strain of *Pseudomonas fluorescens* and showed limited gravitational settling. Therefore, iron (Fe) and aluminum (Al) sacrificial electrodes were used in a batch reactor under galvanostatic conditions. The best Se(0) turbidity removal (97 %) was achieved using iron electrodes at 200 mA. Aluminum electrodes removed 96 % of colloidal Se(0) only at a higher current intensity (300 mA). At the best Se(0) removal efficiency, electrocoagulation using Fe electrode removed 93 % of the Se concentration, whereas with Al electrodes the Se removal efficiency reached only 54 %. Due to the less compact nature of the Al flocs, the Se-Al sediment was three times more voluminous than the Se-Fe sediment. The toxicity characteristic leaching procedure (TCLP) test showed that the Fe-Se sediment released Se below the regulatory level ( $1 \text{ mg L}^{-1}$ ), whereas the Se concentration leached from the Al-Se sediment exceeded the limit by about 20 times. This might be related to the mineralogical nature of the sediments. Electron scanning micrographs

showed Fe-Se sediments with a reticular structure, whereas the Al-Se sediments lacked an organized structure. Overall, the results obtained showed that the use of Fe electrodes as soluble anode in electrocoagulation constitutes a better option than Al electrodes for the electrochemical sedimentation of colloidal Se(0).

**Keywords** Elemental selenium · Colloids · Electrocoagulation · Aluminum electrodes · Iron electrodes · TCLP

## Introduction

Selenium (Se) has a complex biogeochemistry with both abiotic and biotic reactions involved in its cycling through different compartments of the environment. The two most oxidized forms, or oxyanions, namely, selenite (Se[IV],  $\text{SeO}_3^{2-}$ ) and selenate (Se[VI],  $\text{SeO}_4^{2-}$ ), are water soluble, bioavailable, and toxic (Simmons and Wallschlaeger 2005). During the mid-1970s, Lake Belews in North Carolina was affected by Se oxyanions released by a coal-fired power plant, which resulted in the massive die-off of the local fish populations: 19 out of 20 species were eliminated (Lemly 2002). In the early 1980s, the Se-laden agricultural drain water discharged in the Kesterson Reservoir, California, severely affected the migratory bird populations and triggered environmental actions (Ohlendorf 1989).

In contrast to its soluble oxyanions, Se (Se(0)) is particulate and less bioavailable (Lenz and Lens 2009). However, when released into surface waters, Se(0) has been reported to adversely affect bivalve mollusks (Luoma et al. 1992; Schlekert et al. 2000) and to be oxidized to Se oxyanions (Zhang et al. 2004). Because the filter-feeding mollusks are situated at the bottom of the trophic network, their Se content is biomagnified in the higher trophic levels (Chapman et al.

---

Responsible editor: Philippe Garrigues

---

L. C. Staicu · P. N. L. Lens  
Department of Environmental Engineering and Water Technology,  
UNESCO-IHE Institute for Water Education, 2601 DA Delft, The  
Netherlands

L. C. Staicu · E. D. van Hullebusch · M. A. Oturan (✉)  
Laboratoire Géomatériaux et Environnement, EA 4508, UPEM,  
Université Paris-Est, 5 bd Descartes, 77454 Mame-la-Vallée, Cedex  
2, France  
e-mail: Mehmet.Oturan@univ-paris-est.fr

E. A. H. Pilon-Smits  
Biology Department, Colorado State University, Fort Collins,  
CO 80523, USA

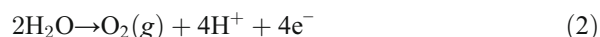
2010). The impact of colloidal elemental Se(0) on bivalve mollusks and trophic networks was investigated extensively in the San Francisco Bay area (Purkerson et al. 2003; Presser and Luoma 2006; EPA 2010; Schlekot et al. 2000). To complicate matters further, biogenic Se(0) exhibits colloidal properties that make its separation from aqueous solution problematic (Buchs et al. 2013; Staicu et al. 2014a).

Major sources of wastewaters containing selenium oxyanions are oil refining industry, coal combustion, and metal refining (Lemly 2004; EPA 2010). The biological treatment of these wastewaters produces different concentration levels of colloidal Se(0) as a function of the initial Se content and the Se conversion rate. Removal of colloidal Se(0) from the bioreactor effluent is necessary to reduce its environmental load and the negative impact exerted on aquatic ecosystems.

During the last decades, electrocoagulation (EC) has gained recognition as a powerful water treatment technology (Holt et al. 2005) to remove colloidal species from water. In EC, the electrical current is applied between two electrodes (including a sacrificial anode) immersed in the (waste)water to be treated. Applying a current across electrodes creates an electrical field and causes the electrolysis of water and the dissolution of sacrificial anode to form a coagulant. The coagulants are thus electrogenerated in situ and in a continuous manner during the application of the process.

The main reactions taking place at the anode and cathode in an electrolytic cell are the following (Mollah et al. 2004):

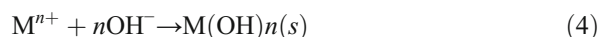
At the anode:



At the cathode:



In the bulk solution:



where M is the metal (e.g. aluminum (Al), iron (Fe)) in its elemental form (zero valence state),  $M^{n+}$  is the oxidized metal ( $n=2, 3$ ),  $ne^{-}$  represents the number of electrons transferred. Due to their proven efficiency and affordable price, Al and Fe electrodes are frequently employed in EC processes. In the case of Fe anode, the  $Fe^{2+}$  ions are oxidized by dissolved  $O_2$  to

form  $Fe^{3+}$  (4). The release of polyvalent cations neutralizes the negatively charged colloidal particles leading to their destabilization and aggregation. In addition, the presence of an electrical field enhances the collision probability and therefore the efficiency of the coagulation process.

Reactions (1) and (4) explain the formation of metallic cations and their hydroxides that react to form hydroxo monomeric and polymeric species. Metal hydroxides have large surface areas involved in the adsorption of soluble and colloidal particles (Mollah et al. 2001). In addition, gas bubbles in the form of oxygen (2) and hydrogen (3) are generated by both electrodes. The gas bubble formation can negatively impact the settling efficiency of the contaminant-metal hydroxide flocs. In order to minimize this effect, lower currents and vertical electrode configurations are suggested (Heidmann and Calmano 2010).

Various electrocoagulation studies have focused on treating toxic metals (Vasudevan et al. 2009; Akbal and Camci 2011; Al Aji et al. 2012; Mello Ferreira et al. 2013; Öncel et al. 2013), turbidity (Trompette et al. 2008; Gamage and Chellam 2011; Khandegar and Saroha 2013), microorganisms (Zhu et al. 2006), or complex organic matrices (Un et al. 2009). Kabdasli et al. (2012) and Vasudevan and Oturan (2014) provide an extensive and in-depth analysis of the wastewater types treated by electrocoagulation. To our best knowledge, there is no study reported in the literature about the elimination of colloidal Se(0) from water by EC. Therefore, the aim of this study was to investigate the viability for the removal of colloidal biogenic Se(0) by EC. Colloidal Se(0) was produced by a strain of *Pseudomonas fluorescens* (Staicu et al. 2014b). Fe and Al electrodes were used as sacrificial anodes. The colloidal Se(0) removal capacity of the system was evaluated using different operating parameters, including current density and electrode type. Coagulation efficiency was determined by turbidity measurements. Furthermore, the residual metal content of the supernatant was determined. The sediments produced at the end of the EC were analyzed in terms of structure and metal leaching behavior.

## Materials and methods

### Reagents and electrodes

For bacterial growth, King B (KB) medium was prepared as described by King et al. (1954). Sodium selenite,  $Na_2SeO_3$ , >99 %, was purchased from Sigma-Aldrich. Coagulant reagent was generated by the electrodisolution of Al (99 % purity) and Fe (99.5 % purity) electrodes both from Goodfellow Ltd., UK.

All solutions were prepared using deionized water. Before and after each experiment, the electrodes were degreased by wiping with an acetone-soaked tissue, abraded with sand

paper, and rinsed with ultrapure water to remove any impurities and oxide layers (Heidmann and Calmano 2010).

### Biogenic elemental Se production and solution preparation

Biogenic elemental Se (Se(0)) was produced aerobically by a strain of *P. fluorescens*, isolated from the roots of *Stanleya pinnata* (family *Brassicaceae*), a model Se hyperaccumulator species (Staicu et al. 2014b). The KB medium was supplemented with 10 mM Na<sub>2</sub>SeO<sub>3</sub> from a filter-sterilized 1 mol L<sup>-1</sup> stock solution and with 1 % (v/v) of *P. fluorescens* inoculum sampled during the mid-logarithmic growth phase. The incubation was performed under aerobic conditions at 28 °C, pH<sub>0</sub>=7.5, and 160 rpm. After 24 h, the incubation turned red, indicative of SeO<sub>3</sub><sup>2-</sup> reduction to red elemental Se. Elemental Se was harvested by centrifugation (at 3200×g for 10 min), washed twice with deionized water, and re-suspended in 42 mM NaCl solution (Canizares et al. 2007). The electrolyte addition corresponded to a conductivity of around 4.5 mS cm<sup>-1</sup>. The turbidity of the solution was adjusted by adding biogenic Se(0) or NaCl solution until the desired target value was reached. Due to the colloidal nature of Se(0) the targeted turbidity value of the suspension was set within ±5 %. NaCl acts as supporting electrolyte.

### Electrocoagulation setup

The coagulating agents were electrogenerated using sacrificial metallic anodes of Al and Fe, respectively (Fig. 1). The electrochemical experiments were conducted under galvanostatic conditions, i.e., the current was set and the potential adjusted its value as a function of system's resistance. The electrocoagulation experiments were carried out in batch mode in a 500-mL single-compartment electrochemical cell containing colloidal Se(0) suspension and two electrodes (100 mm height×50 mm width×1 mm thick in dimension with 6 cm depth in solution). Both the anode and the cathode are consisting of same metal (Al or Fe). The electrodes were connected in a monopolar mode and were placed vertically and parallel to each other. This electrode configuration was chosen to minimize the flotation effect of the hydrogen and oxygen gas bubble evolution exerted on the colloidal Se(0) suspension. The conversion between the applied current (*I*) and the current density *J* ( $J=I/A$ , with *A* surface area) is presented in Table 1. For ease of comparison between datasets, we employed the current values for generating the graphs.

In order to improve the mass transfer, the electrochemical reactor was mixed at 300 rpm using a 3-cm magnetic stir bar. The electrodes were immersed in the solution up to a 60-cm<sup>2</sup> active electrode geometric area with a 3-cm electrode gap. The constant agitation produced by the magnetic stir bar ensured the homogeneous mass transfer of the coagulant within the electrochemical reactor and increased the collision frequency

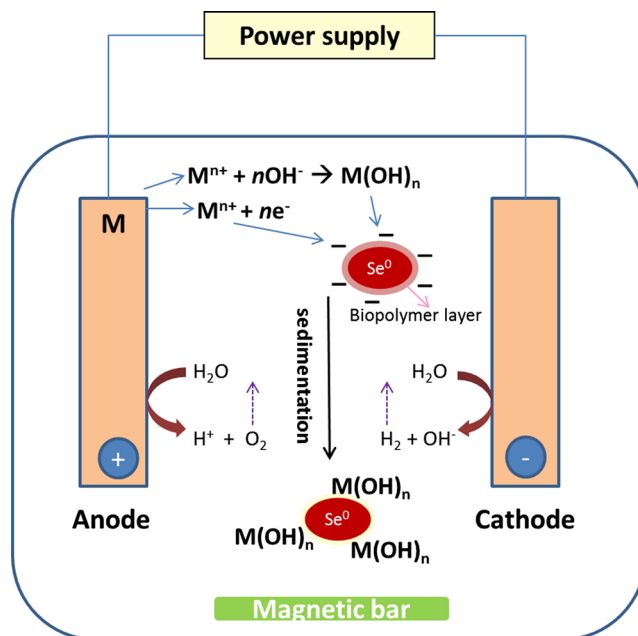


**Fig. 1** Schematic diagram of the electrocoagulation setup. *M*=metal (e.g. Al, Fe), *n*<sup>+</sup>=oxidation state; *M(OH)<sub>n</sub>*=metal hydroxides

of colloidal Se(0) particles with the coagulating agent. Based on a preliminary study (data not shown), we determined the optimal distance to be 3 cm and the optimal stirring speed to be 300 rpm. The distance between electrodes is a critical parameter in the electrochemical cell design since a suboptimal electrode gap increases the IR-drop leading to higher energy consumption (Mollah et al. 2004). The results are presented as average values of three independent experiments (triplicates, *n*=3) unless otherwise stated. When the standard deviation values were smaller than 5 %, the error bars were not represented. All data was analyzed by using the data analysis software SigmaPlot 12.0v.

### Electrocoagulant generation

In order to determine the amount of Al and Fe electrogenerated, separate experiments were performed. The Se(0)-free solution contained 42 mM NaCl and the sampling was done with the same frequency as the EC Se(0) treatment protocol. All samples were acidified with 65 % HNO<sub>3</sub> and stored at 4 °C until elemental analysis was performed on a PerkinElmer Optima 8300 Inductively Coupled Plasma-Optical Emission Spectroscopy (ICP-OES). Residual Se, Fe, and Al were determined by the same method. Calibration standards were prepared by stepwise dilution of a multi-element ICP standard solution (Merck, Darmstadt, Germany). The wavelengths employed were 196.026 nm for Se, 238.204 nm for Fe, and 396.153 nm for Al, respectively. At the end of the sedimentation stage, the supernatants were carefully siphoned from the sedimentation cones. Both the supernatant and the sediments were collected for further analyses.

**Table 1** Summary of the EC results using Al and Fe sacrificial electrodes

<i>I</i> (mA)	<i>j</i> (mA cm <sup>-2</sup> )	<i>U</i> (V)	Removal efficiency (%)	Residual turbidity (NTU)	Fe <sub>theo</sub> (g L <sup>-1</sup> )	Al <sub>theo</sub> (g L <sup>-1</sup> )	<i>E</i> (kWh m <sup>-3</sup> )	<i>C</i> <sub>electrode</sub> (kg m <sup>-3</sup> )	<i>M</i> <sub>sediment</sub> (kg m <sup>-3</sup> )
Fe electrodes									
50	0.83	1.4	69	157	0.1		0.14	0.104	17.4
100	1.67	2.3	81	95	0.21		0.46	0.208	39.2
200	3.33	3.9	97	16	0.42		1.56	0.417	61.6
300	5.00	5.1	97	18	0.63		3.06	0.625	71.8
500	8.33	7.9	96	20	1.04		7.9	1.042	84.5
Al electrodes									
50	0.83	1.9	71	151		0.03	0.19	0.034	32
100	1.67	2.6	86	86		0.07	0.52	0.067	76
200	3.33	4.2	88	61		0.13	1.68	0.134	150
300	5.00	5.7	96	22		0.2	3.42	0.201	212
500	8.33	8.5	95	25		0.33	8.5	0.336	376

Fe theoretical Fe<sub>theo</sub> (mg L<sup>-1</sup>), Al theoretical Al<sub>theo</sub> (mg L<sup>-1</sup>), electrical energy consumption *E* (kWh m<sup>-3</sup>), electrode consumption *C*<sub>electrode</sub> (kg m<sup>-3</sup>), and mass of sediment *M*<sub>sediment</sub> (kg m<sup>-3</sup>) were determined after 60 min of electrolysis

### Toxicity characteristic leaching procedure test

The sediment samples were analyzed using the toxicity characteristic leaching procedure (TCLP) performed according to the testing guidelines specified by the US Environmental Protection Agency (USEPA 1999). The sediment was mixed in a glacial acetic acid (of 99.5 % assay) solution at 1:20 with a final pH of 2.88±0.05. The leachate mixture was sealed in the extraction vessel (plastic centrifuge tubes, 29×115 mm, 50 mL) and tumbled for 20 h using a Grant Bio PTR-30 360° Vertical Multi-Function Rotator to simulate an extended leaching time in the ground. The vertical rotation speed employed was 30 rpm. After 20 h, the samples were filtered gravitationally through Whatman glass microfiber filters, grade GF/F (0.7 μm cutoff) and the filtrate analyzed by ICP-OES.

### Analytical methods

Turbidity was measured using a HACH 2100P ISO turbidimeter (Hach 2100P ISO) containing a T860-nm LED lamp and was expressed in nephelometric turbidity units (NTU). Fifteen-milliliter aliquots were sampled according to the manufacturer's instructions. Electrophoretic mobility measurements were performed on a Zetasizer Nano ZS (Malvern Instrument Ltd., Worcestershire, UK) using a laser beam at 633 nm and a scattering angle of 173° at 25 °C according to the manufacturer's instructions. The volume of settled Se(0) was measured in standard 1000-mL Imhoff graduated cones (USEPA 1999).

Environmental scanning electron microscopy (ESEM, ELECTROSCAN E3, Hillsboro, OR, USA) was used for the observation of the microstructure of Se-Fe and Se-Al sediments. ESEM allows the examination of wet specimens

without sample preparation (Donald 2003). The samples were observed at 25 kV. X-ray diffraction (XRD) analysis was performed on a Bruker D8 Advance diffractometer (Karlsruhe, Germany) equipped with an energy dispersion Sol-X detector with copper radiation (CuKα, λ=0.15406 nm). The acquisition was recorded between 10° and 80°, with a 0.02° scan step and 1-s step time.

pH was measured by an EUTECH 1500 pH meter. Conductivity measurements were performed on a Radiometer Analytical MeterLab CDM 230. The electrical current was applied and the evolution of the current and voltage was monitored using a HAMEG Triple Power HM7042-5 (Mainhausen, Germany).

### Calculations

The specific electrical energy consumption *E* (kWh m<sup>-3</sup>) for turbidity removal was calculated as follows (Heidmann and Calmano 2010):

$$E = \frac{U \cdot I \cdot t}{V \cdot 1000} \quad (5)$$

where *U* is the required voltage (V), *I* the applied current (A), *t* electrolysis time (h), and *V* the volume of the treated solution (m<sup>3</sup>).

The maximum possible mass of Al and Fe electrochemically generated from sacrificial anodes for a particular electrical current was calculated using Faraday's law of electrolysis (Mechelhoff et al. 2013):

$$m = \frac{j \cdot A_{el} \cdot M \cdot t}{V \cdot z \cdot F} \quad (6)$$

where  $m$  is the mass of the anode material dissolved (g),  $j$  the current density ( $A\ m^{-2}$ ),  $A_{el}$  the active electrode area ( $m^2$ ),  $M$  the molar mass of the anode material ( $g\ mol^{-1}$ ),  $t$  electrolysis time (s),  $V$  volume of the reactor ( $m^3$ ),  $z$  the number of electrons transferred, and  $F$  the Faraday's constant ( $96,485\ C\ mol^{-1}$ ). The cathode dissolution was not considered.

## Results and discussion

### Characterization of the biogenic Se(0) suspension

The colloidal stability of biogenic Se(0) is presented in Fig. 2a. Biogenic Se(0) displayed limited sedimentation during the 4-day study interval, from 500 to 420 NTU, corresponding to a normalized removal of 0.16. Note that turbidity was normalized against its initial value using a scale from 0 to 1 (1 represents no sedimentation and 0 represents total sedimentation of the colloidal system). The colloidal stability of Se(0) is related to the negatively charged biopolymers that are coating the biogenic selenium particles (Dobias et al. 2011; Buchs et al. 2013).

The properties of the biogenic red Se(0) solution (Fig. 2b) are summarized in Table 2. The suspension is characterized by high turbidity and neutral pH. The Se(0) particles exhibit a negative surface charge of around  $-20\ mV$ .

### Electrodissolution of the Al and Fe electrodes

Figure 3 compares the variation of the concentrations of electrogenerated Al and Fe measured with respect to the electrical charge passed. For both electrodes, the metal concentration increases linearly with the electrical charge. The measured values exceed the predicted values calculated from Eq. (6), i.e., a super-faradaic yield is obtained. In the case of Al, the difference is negligible, whereas the Fe anode exhibits 1.3 times higher measured concentrations than the theoretically expected ones. Even if Fe has a higher redox potential ( $-0.44\ V$ ) than Al ( $-1.67\ V$ ), the formation of an Al oxide layer during electrolysis coats the electrode surface, thus decreasing its corrosion potential (Roberge 2008).

The super-faradaic yield exhibited by the Fe electrodes could be explained by the difference between the electrode's geometric area and the actual area that takes into account the surface roughness. Electrocoagulation is corroding the sacrificial anodes, thus increasing their surface area as a function of the anode material, the current applied, and the corrosiveness of the solution (Roberge 2008). An alternative explanation considers the additional chemical dissolution of the Fe anode (Canizares et al. 2005) due to corrosion. In addition, Picard et al. (2000) reported cathodic dissolution as a consequence of the chemical attack by the hydroxyl ions released during water

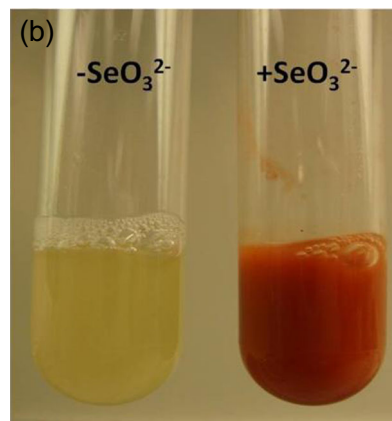
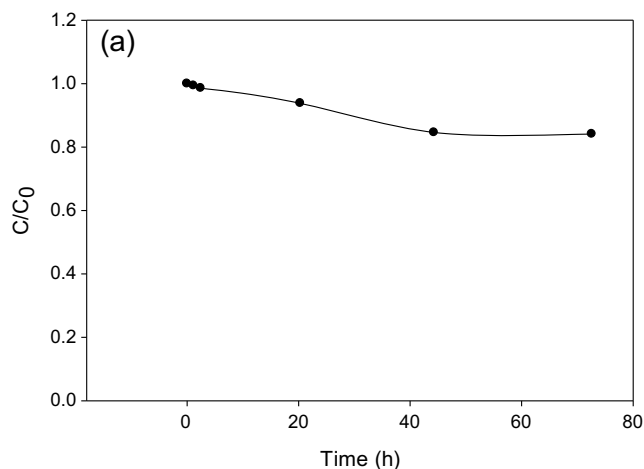


**Fig. 2** a Colloidal stability of biogenic red Se(0) produced by *P. fluorescens*. Evolution of the ratio  $C/C_0$  in function of treatment time with  $C_0$  and  $C$  the turbidity (in NTU) at the initial and a giving time, respectively, and **b** biogenic red Se(0) produced by *P. fluorescens* and the control sample (KB medium)

electrolysis. However, they used a very high conductivity ( $0.6\ mol\ L^{-1}\ NaCl$ ) and the currents used were 200 times higher than those applied in the current study.

### Treatment efficiency of electrocoagulation

#### Turbidity removal

Figure 4a compares the turbidity removal using Fe and Al anodes as a function of the current intensity. For the first two

**Table 2** Properties of biogenic Se(0) solution produced by a *P. fluorescens* strain (growth conditions:  $28\ ^\circ C$ ; 160 rpm;  $pH_0 = 7.5$ ; aerobic; incubation time, 24 h)

Parameter	Value
Turbidity (NTU)	$500 \pm 30$
Se ( $mg\ L^{-1}$ )	$310 \pm 12$
Color	Red
pH	$7.0 \pm 0.2$
Conductivity ( $mS\ cm^{-1}$ )	$4.5 \pm 0.2$
Zeta potential (mV)	$-20 \pm 2$

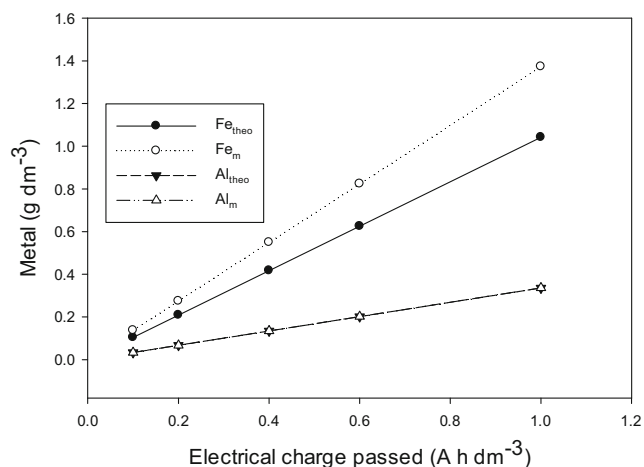


**Fig. 3** Variation of theoretical and measured Al and Fe with the electrical charge passed during EC. Operating conditions: temperature, 20 °C; volume, 0.5 L; supporting media, 42 mmol L<sup>-1</sup> of NaCl; pH<sub>0</sub>=7.0; 300 rpm; electrolysis time, 60 min. Fe<sub>theo</sub> and Al<sub>theo</sub> refer to the theoretical metal dissolved according to Faraday's law (Eq. (6)). Fe<sub>m</sub> and Al<sub>m</sub> are the measured values with charge passed

current values applied (50 and 100 mA), the Al electrodes produced a slightly higher turbidity removal than the Fe electrodes. At 50 and 100 mA, the Al electrodes removed 71 and 86 % of the initial turbidity, whereas the Fe electrodes achieved 69 and 81 %, respectively. In contrast, Fe electrodes lead to a better turbidity removal at higher applied current intensity values. For example, when increasing the current to 200 mA, the Fe electrodes produced the highest turbidity removal (97 %). At the same current, Al generated only 88 % turbidity removal. Above 200 mA, the electrodes displayed different trends. While turbidity removal by the Fe electrodes remained almost constant at around 97 % for 300 and 500 mA, Al showed the highest performance at 300 mA, with 96 % removal efficiency, followed by 95 % removal at 500 mA. Overall, these results indicate a plateau above 200 mA for the Fe electrodes and above 300 mA for the Al electrodes.

Because colloids and electrically charged ions are held in suspension due to the electrostatic repulsion forces, the presence of counter ions brings about neutralization of the electric charge and diminishes their colloidal stability (Khandegar and Saroha 2013). On the other hand, when liberated in the bulk solution, the metal cations hydrolyze spontaneously by forming a series of metastable hydrolysis products that transit towards thermodynamically stable metal hydroxides (Richens 1997). Destabilized colloidal particles are adsorbed onto metal (oxy)hydroxides or followed by precipitation (Hanai and Hasar 2011). As a consequence of these mechanisms, the colloids aggregate and settle down.

The relation between the current applied and the turbidity removal was not linear (Fig. 4a). This indicates a decrease of current efficiency during the electrolysis time, either due to parasitic reactions that are enhanced with the increase of the

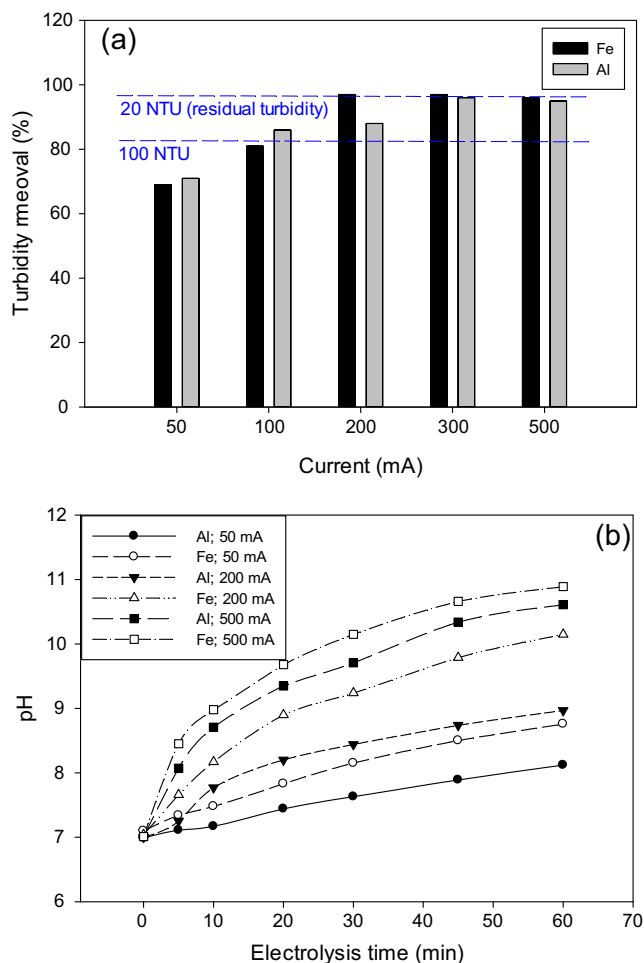


**Fig. 4** **a** Turbidity removal. **b** pH evolution for Fe and Al electrodes. Note that the *dashed lines* in panel (**a**) represent residual turbidity (NTU). Operating conditions: temperature, 20 °C; volume, 0.5 L; supporting electrolyte, 42 mmol L<sup>-1</sup> of NaCl; pH<sub>0</sub>=7.0; 300 rpm; electrolysis time, 60 min

applied current or to the formation of a passivation layer. Since the temperature measured during the experiments increased only marginally (less than 0.5 °C) compared to the beginning of the experiment, the Joule effect (i.e., heating induced by the increase of the applied current) seems not to play an important role (Kabdasi et al. 2012). Passivation of the electrode surface has been shown to affect the performance of the process (Mouedhen et al. 2008; Lakshmanan et al. 2009). Because the highest removal efficiencies were recorded at the beginning of the plateau, no further experiments were performed at currents above 500 mA.

pH is an important factor that influences the speciation of Fe and Al during the process (Mollah et al. 2001). Figure 4b shows the pH evolution during electrolysis time as a function of the applied current. All experiments started at a pH value of 7.0±0.2. For each current intensity tested, the Fe electrodes induced a higher pH increase than the Al ones. It is important to note that the pH has an important contribution to the formation of Fe and Al hydroxides. During experiments with

Fe electrodes, the net increase of pH for all current densities resulted in the formation of dark-colored sediments indicative of the presence of ferric hydroxide deposits (results not shown).

Several mechanisms of colloidal particles destabilization and sedimentation have been proposed (Duan and Gregory 2003). Turbidity removal by sweep flocculation acts by entrapping and bridging the colloids in a floc with the subsequent sedimentation (Mollah et al. 2004). In addition, charge repression of the electrical double layer of the colloidal particles can play a role by diminishing the repulsion potential between likely charged particles. As a consequence, the particles clump together and settle (Duan and Gregory 2003). Based on the evolution of the pH during EC experiments, it is likely that sweep flocculation had an important contribution to the overall sedimentation process.

In a previous study (Staicu et al. 2014a), we showed that biogenic Se(0) produced by an anaerobic mixed microbial culture exhibits high colloidal stability that can be repressed by using metal hydrolyzing salts in a chemical coagulation (CC) approach. The biogenic Se(0) suspension used in the two studies had different sources (pure aerobic *Pseudomonas* versus mixed anaerobic microbial cultures). In addition, the two suspensions displayed different characteristics: the biogenic Se(0) suspension produced by the mixed culture had a 300 NTU higher turbidity and zeta potential of  $-23 \pm 3$  mV at pH 7.0, the pH decreased with the addition of metallic salts from pH 8 to 7, and the solution contained by-products of bacterial metabolism. It is interesting to note though that the chemical-dosing study (Staicu et al. 2014a) indicates maximum turbidity removal efficiencies at metal ion doses significantly lower than those electrogenerated in EC. In the case of treatment with Al salts,  $0.12 \text{ mg L}^{-1}$  Al dosed as aluminum sulfate achieved 92 % turbidity removal, while in EC, the maximum turbidity removal of 96 % was obtained by electrogenerating  $420 \text{ mg L}^{-1}$  Al. On the other hand, for treatment with Fe salts,  $0.167 \text{ mg L}^{-1}$  were needed in CC to achieved 43 % turbidity removal, versus  $200 \text{ mg L}^{-1}$  of electrogenerated Fe induced 97 % turbidity removal. Metal speciation as a function of pH as well as the floc growth and the interaction between metals and biopolymers and organic molecules could explain the differences between the performances of the two approaches (Holt et al. 2002).

*TCLP and supernatant characterization*

Leaching tests of the electrogenerated Al and Fe sediments were conducted following the TCLP method (US EPA Method 1311). The sediments generated by 50- and 100-mA currents were investigated in terms of the amount of Se, Fe, and Al released from the sediment matrix. Figure 5a presents the TCLP results of Se-Fe and Se-Al sediment samples. At 50 mA, the Se-Al sediment released 5 times more Se than the

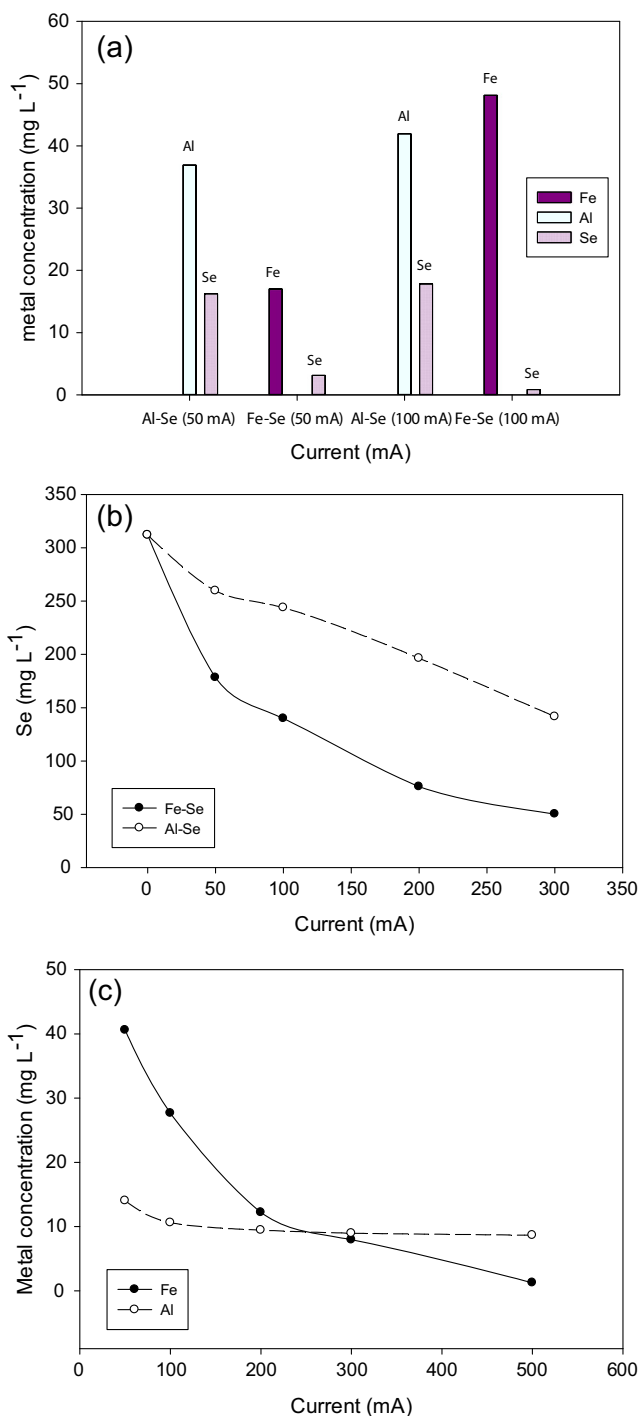


**Fig. 5** a TCLP of Se-Al and Se-Fe sediments, b residual Se in the supernatant of Al and Fe electrode experiments. Note that “0 mA” corresponds to the initial Se content of the suspension before EC treatment, and c residual Al and Fe from the supernatant of Al and Fe electrode experiments. Note that “0 mA” corresponds to the initial Se content of the suspension before EC treatment

Se-Fe sample,  $16 \text{ mg L}^{-1}$  versus  $3 \text{ mg L}^{-1}$ . When doubling the applied current, the difference between the Se released by the two sediments increased 22 times:  $17.8$  versus  $0.8 \text{ mg L}^{-1}$ . Only the Se concentration of the leachate from the Se-Fe

sediment generated at 100 mA complied with the  $1 \text{ mg L}^{-1}$  EPA regulatory limit (US EPA Method 1311).

Al-Se and Fe-Se sediments showed different leaching behavior of Al, Fe, and Se, respectively. At 50 mA, the concentration of Al released was twofold higher than the Fe concentration, whereas at 100 mA, the Al concentration was slightly inferior compared to the Fe concentration. Fe and Al are not TCLP-regulated elements (US EPA Method 1311 Chapter). The stability of sediments over time is an open question related to the validity of the TCLP approach as a tool for the sound characterization of the leaching potential of sediments to be landfilled.

Residual turbidity (Fig. 4a) is an important parameter in wastewater treatment. Low residual turbidity is desirable from a technological and ecotoxicological standpoint. The lowest turbidity achieved by the Fe electrodes was 16 NTU for

200 mA. The Al electrodes achieved a minimum residual turbidity of 22 NTU at 300 mA. While in chemical coagulation, the addition of the coagulant is a discrete event and the system shifts towards a final equilibrium state, in EC, the equilibrium is constantly moving. Therefore, trying to determine the turbidity removal kinetics in EC is challenging because of the concomitant formation of metal hydroxides during electrolysis that add to the overall turbidity (Holt et al. 2002).

Residual Se (total selenium) remaining in the supernatant after the liquid–solid phase separation is presented in Fig. 5b. The initial Se concentration of the colloidal Se(0) solution ( $500 \pm 30 \text{ NTU}$ ) was  $310 \pm 12 \text{ mg L}^{-1}$ . Residual Se (total) varies with the current intensity and the electrode type used. For all current intensities, the Fe electrode as sacrificial anode is more efficient in Se removal than the Al electrode. The

**Fig. 6** Sediment analysis. ESEM micrographs of **a** Se-Al sediment (500-nm scale), **b** Se-Fe sediment (500-nm scale), **c** XRD diffractogram of Se-Al sediment, **d** XRD diffractogram of Se-Fe sediment, and **e** evolution of Al-Se and Fe-Se sediment volume. The sediments analyzed were produced at 100 mA under the following conditions (Se(0) turbidity, 500 NTU; temperature, 20 °C; supporting media,  $42 \text{ mmol L}^{-1} \text{ NaCl}$ ;  $\text{pH}_0=7.0$ ; 300 rpm; electrolysis time, 60 min). Note that the volume of the treated solution was 500 mL

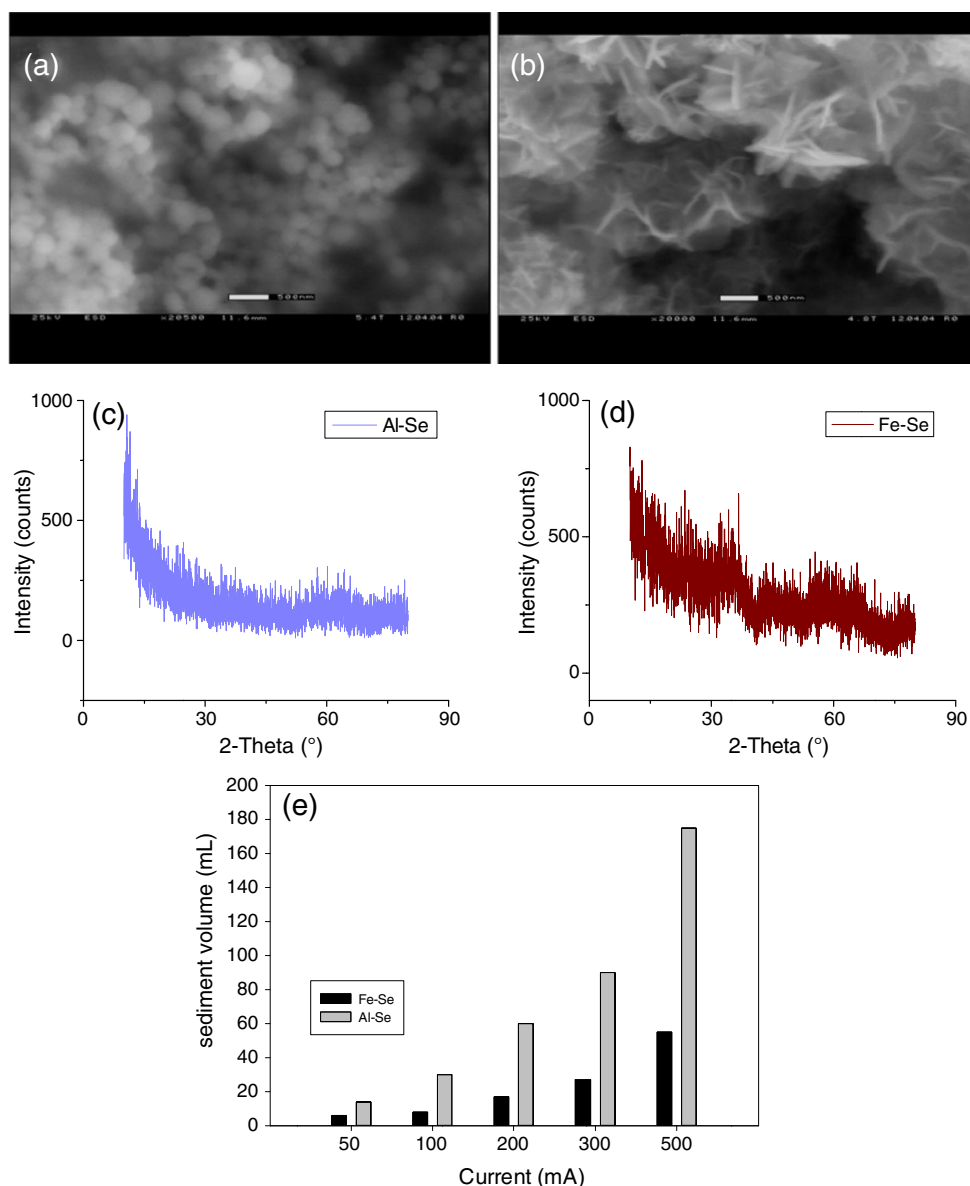


**Table 3** Summary of Se-Fe and Se-Al sediment characteristics

	<i>I</i> (A)	Volume (mL) <sup>a</sup>	Volume (mL) <sup>b</sup>	Mass (g) <sup>a</sup>	Mass (g) <sup>b</sup>	Density (g/mL) <sup>a</sup>	Density (g/mL) <sup>b</sup>
	0.05	5	11	9	16	1.74	1.45
	0.1	12	28	20	38	1.64	1.36
	0.2	24	58	31	75	1.28	1.29
	0.3	31	82	36	106	1.16	1.29
<sup>a</sup> Fe-Se sediment	0.5	38	170	42	188	1.11	1.11
<sup>b</sup> Al-Se sediment							

minimum Se concentration (141.6 mg L<sup>-1</sup>) in the Al electrode experiment was recorded at 300 mA, corresponding to around 54 % Se reduction. In contrast, at 500 mA, the Fe anode decreased the total Se concentration up to 23 mg L<sup>-1</sup> which corresponds to a Se removal efficiency of around 93 %. By comparing the two electrodes, the Fe was almost six times more efficient than Al in total Se removal from analysis of the supernatant of the electrocoagulation cell upon termination of the experiment.

Figure 5c displays the residual total Al and Fe concentrations present in the supernatant at the end of the sedimentation stage. While the Fe concentration decreased with the applied current, from 41 mg L<sup>-1</sup> (at 50 mA) to 1.26 mg L<sup>-1</sup> at 500 mA, the Al concentration showed a limited decrease with the applied current, from 14.2 mg L<sup>-1</sup> (at 50 mA) to 8.64 mg L<sup>-1</sup> (at 500 mA). The decrease in Fe concentration can be linked to the decrease in residual Se because Fe (oxy)hydroxides co-precipitate with colloidal Se(0) and is entrapped in the sediment. The higher Se concentration in the Al electrode experiment could also be understood in the same framework.

Secondary pollution refers to pollutants that are not initially present in the wastewater but are introduced during treatment. EC adds the anode-corroded metal to the treated solution. A drawback of using Fe electrodes in EC is related to the residual color (yellowish, green, greenish-black) produced by the dissolution and speciation of Fe (Moreno et al. 2009). It is generally agreed that Al is not required for proper functioning of biological systems (Gensemer and Playle 1999) and therefore, its presence can elicit toxic effects. In contrast, Fe is an essential metabolic component functioning as a cofactor in a wide array of proteins and enzymes (Arredondo and Nunez 2005). Dong et al. (2014) investigated the comparative toxicity potentials (CTP) of 14 cationic metals, including Al and Fe, in freshwater environments. While Al had one of the highest CTP, Fe ranked among the metals with the lowest CTP. Therefore, from an ecotoxicological standpoint, Fe is a better option for treating colloidal Se(0) suspensions.

**Sediment characterization**

To clarify the structure of sediments, we carried out ESEM micrographs of Se-Al and Se-Fe sediments. Results obtained are depicted on Fig. 6a, b. Se-Al does not appear to have an

organized structure. Se(0) nanoparticles are clearly visible. In contrast, the Se-Fe sediment shows a reticular structure with no observable Se(0) particles.

X-ray diffraction was performed to investigate the mineralogy of the two types of sediments (Fig. 6c, d). Gamage and Chellam (2011) reported that Al sediments generated by EC having an amorphous state and a gelatinous appearance. The same observation was made for our samples (results not shown). The diffractogram of Se-Fe sediments (Fig. 6d) also indicates an amorphous state. This result is in agreement with that reported by Heidmann and Calmano (2010) concerning iron-based sediments generated by EC.

The properties of Se-Fe and Se-Al sediments generated by electrocoagulation using different currents are summarized in Table 1. On the other side, the evolution of Se-Fe and Se-Al sediment volume as a function of the applied current can be seen in Fig. 6e. While the volume of both Al and Fe sediments show a positive trend with the increase in current, the Se-Al sediment becomes more voluminous than Se-Fe by a factor of 2 (at 50 mA) to 4.5 (at 500 mA). Because Fe and Al have different densities (7.874 and 2.70 g cm<sup>-3</sup> for Fe and Al, respectively) this will impact the floc and eventually sediment structure (Lide 2004; Turchiuli and Fargues 2004). Moreover, higher currents have been shown to increase the bubble densities and create Al flocs with a less compact structure (Holt et al. 2002). Al flocs produced in EC are fragile and relatively porous, therefore prone to breakage (Harif et al. 2012). Smaller flocs thus created are characterized by a poor settleability and voluminous sediment with a porous structure (Harif and Adin 2011). The size of the flocs can play a significant role in

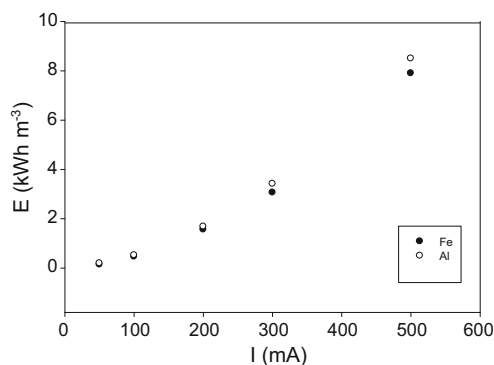


**Fig. 7** Electrical energy consumption in EC of Se(0) with Al or Fe electrodes

settling and solid–liquid separation as well as in the structure of the sediment (Jarvis et al. 2005).

The mass of the Se-Fe and Se-Al sediments is superior to their volume, resulting in a density greater than unity (Table 3). The difference in mass between the two sediments mirrors their difference in volume.

#### Electrical energy consumption and process optimization

The electrical energy consumption by the two kinds of electrodes is depicted on Fig. 7. As can be seen in Table 3, for the first three applied currents, 50, 100, and 200 mA, Al and Fe electrodes had almost similar electrical energy consumption (below  $1.68 \text{ kWh m}^{-3}$ ). Above 200 mA, at the highest turbidity removal efficiencies, Al electrodes showed a higher energy consumption than Fe ( $3.42 \text{ kWh m}^{-3}$  versus  $1.5 \text{ kWh m}^{-3}$ ).

Table 3 shows the importance of the process optimization. Using currents above the optimal value led to higher electrode consumption and more sediment generated. At the optimum Se(0) removal currents, Fe electrodes lost two times more of their mass comparing to Al electrodes:  $0.417$  versus  $0.201 \text{ kg m}^{-3}$ . On the other hand, the resulting Se-Al sediment ( $212 \text{ kg m}^{-3}$ ) was 3.4 times higher in weight than the Se-Fe sediment ( $61.6 \text{ kg m}^{-3}$ ). These contrasting results could be explained by the flocculation process (floc growth) which entraps water molecules within the metal-Se(0)-biopolymer matrix. Process optimization is thus a particularly important aspect when treating large volumes of Se(0) laden suspensions in a full-scale EC application.

#### Conclusions

From the results obtained in this work, the following conclusions can be drawn:

- Biogenic colloidal Se(0) can be effectively separated from aqueous solution by an electrocoagulation process using Fe or Al electrodes.
- Electrocoagulation with Al and Fe sacrificial electrodes (as anode) can achieve high (up to 97 % with) removal efficiencies of colloidal Se(0).
- Low amounts of electrical energy (below  $4 \text{ kWh m}^{-3}$ ) are consumed during EC of colloidal Se(0). Al electrodes consume twice the amount of energy required by the Fe electrodes to achieve comparable Se(0) removal efficiencies.
- At the highest colloidal Se(0) removal efficiency, the Fe electrodes are consumed two times faster than the Al electrodes. However, the resulted Se-Al sediment is 3.4 times more voluminous than the Se-Fe sediment.

- The TLCP of Se-Fe sediments suggest that the sediment can be listed as non-hazardous waste, whereas the Se-Al sediment exceeded the TCLP limit for Se by almost 20 times.

**Acknowledgments** The authors would like to thank the European Commission for providing financial support through the Erasmus Mundus Joint Doctorate Programme ETeCoS<sup>3</sup> (Environmental Technologies for Contaminated Solids, Soils and Sediments) under the grant agreement FPA no. 2010-0009. A special thanks to Dr. David Huguenot and Dr. Rossana Combes for their respective ICP-OES and ESEM expert technical assistance. The analytical part (ICP-OES) was supported by a grant of the Region Ile de France.

#### References

- Akbal F, Camci S (2011) Copper, chromium and nickel removal from metal plating wastewater by electrocoagulation. *Desalination* 269(1–3):214–222
- Al Aji B, Yavuz Y, Koparal AS (2012) Electrocoagulation of heavy metals containing model wastewater using monopolar iron electrodes. *Sep Purif Technol* 86:248–254
- Arredondo M, Nunez MT (2005) Iron and copper metabolism. *Mol Asp Med* 26:313–327
- Buchs B, Evangelou MWH, Winkel LHE, Lenz M (2013) Colloidal properties of nanoparticulate biogenic selenium govern environmental fate and bioremediation effectiveness. *Environ Sci Technol* 47(5):2401–2407
- Canizares P, Carmona M, Lobato J, Martinez F, Rodrigo MA (2005) Electrodissolution of aluminum electrodes in electrocoagulation processes. *Ind Eng Chem Res* 44:4178–4185
- Canizares P, Martinez F, Jimenez C, Lobato J, Rodrigo MA (2007) Coagulation and electrocoagulation of wastes polluted with colloids. *Sep Sci Technol* 42:2157–2175
- Chapman PM, Adams WJ, Brooks M, Delos CG, Luoma SN, Maher WA, Ohlendorf HM, Presser TS, Shaw P (2010) Ecological assessment of selenium in the aquatic environments. SETAC Press, Pensacola
- Dobias J, Suvorova EI, Bernier-Latmani R (2011) Role of proteins in controlling selenium nanoparticle size. *Nanotechnology* 22(19):195605
- Donald AM (2003) The use of environmental scanning electron microscopy for imaging wet and insulating materials. *Nat Mater* 2:511–513
- Dong Y, Gandhi N, Hauschild MZ (2014) Development of comparative toxicity potentials of 14 cationic metals in freshwater. *Chemosphere* 112:26–33
- Duan J, Gregory J (2003) Coagulation by hydrolyzing metal salts. *Adv Colloid Interf* 100–102:475–502
- Gamage NP, Chellam S (2011) Aluminum electrocoagulation pretreatment reduces fouling during surface water microfiltration. *J Membr Sci* 379:97–105
- Gensemer RW, Playle RC (1999) The bioavailability and toxicity of aluminum in aquatic environments. *Crit Rev Environ Sci Technol* 29(4):315–450
- Hanai O, Hasar H (2011) Effect of anions on removing  $\text{Cu}^{2+}$ ,  $\text{Mn}^{2+}$  and  $\text{Zn}^{2+}$  in electrocoagulation process using aluminum electrodes. *J Hazard Mater* 189:572–576
- Harif T, Adin A (2011) Size and structure evolution of kaolin- $\text{Al}(\text{OH})_3$  flocs in the electroflocculation process: a study using static light scattering. *Water Res* 45:6195–6206
- Harif T, Khai M, Adin A (2012) Electrocoagulation versus chemical coagulation: coagulation/flocculation mechanisms and resulting floc characteristics. *Water Res* 46:3177–3188

- Heidmann I, Calmano W (2010) Removal of Ni, Cu and Cr from a galvanic wastewater in an electrocoagulation system with Fe- and Al-electrodes. *Sep Purif Technol* 71:308–314
- Holt PK, Barton GW, Wark M, Mitchell CA (2002) A quantitative comparison between chemical dosing and electrocoagulation. *Colloid Surface A* 211:233–248
- Holt PK, Barton GW, Mitchell CA (2005) The future of electrocoagulation as a localized water treatment technology. *Chemosphere* 59:335–367
- Jarvis P, Jefferson B, Gregory J, Parsons SA (2005) A review of floc strength and breakage. *Water Res* 39:3121–3137
- Kabdassli I, Arslan-Alaton I, Olmez-Hanci T, Tunai O (2012) Electrocoagulation applications for industrial wastewaters: a critical review. *Environ Technol Rev* 1:2–45
- Khandegar V, Saroha AK (2013) Electrocoagulation for the treatment of textile industry effluent—a review. *J Environ Manag* 128:949–963
- King EO, Ward MK, Raney DE (1954) Two simple media for the demonstration of pyocyanin and fluorescein. *J Lab Clin Med* 44:301–307
- Lakshmanan D, Clifford DA, Samanta G (2009) Ferrous and ferric ion generation during iron electrocoagulation. *Environ Sci Technol* 43:3853–3859
- Lemly AD (2002) Symptoms and implications of selenium toxicity in fish: the Belews Lake case example. *Aquat Toxicol* 57(1–2):39–49
- Lemly AD (2004) Aquatic selenium pollution is a global environmental safety issue. *Ecotoxicol Environ Saf* 59:44–56
- Lenz M, Lens PNL (2009) The essential toxin: the changing perception of selenium in environmental sciences. *Sci Total Environ* 407:3620–3622
- Lide DR (2004) CRC handbook of chemistry and physics, 84th edn. CRC Press, Boca Raton
- Luoma SN, Johns C, Fisher NS, Steinberg NA, Oremland RS, Reinfelder JR (1992) Determination of selenium bioavailability to a bivalve from particulate and solute pathways. *Environ Sci Technol* 26:485–491
- Mechelhoff M, Kelsall GH, Graham NJD (2013) Super-faradaic charge yields for aluminum dissolution in neutral aqueous solutions. *Chem Eng Sci* 95:353–359
- Mello Ferreira A, Marchesiello M, Thivel PX (2013) Removal of copper, zinc and nickel present in natural water containing  $\text{Ca}^{2+}$  and  $\text{HCO}_3^-$  ions by electrocoagulation. *Sep Purif Technol* 107:109–117
- Mollah MYA, Schennach R, Parga J, Cocke DL (2001) Electrocoagulation (EC)—science and applications. *J Hazard Mater B* 84:29–41
- Mollah MYA, Morkovsky P, Gomes JAG, Kesmez M, Parga J, Cocke DL (2004) Fundamental, present and future perspectives of electrocoagulation. *J Hazard Mater* 114:199–210
- Moreno CHA, Cocke DL, Gomes JAG, Morkovsky P, Parga JR, Peterson E, Garcia C (2009) Electrochemical reactions for electrocoagulation using iron electrodes. *Ind Eng Chem Res* 48:2275–2282
- Mouedhen G, Feki M, Wery MDP, Ayedi HF (2008) Behavior of aluminum electrodes in electrocoagulation process. *J Hazard Mater* 150:124–135
- Ohlendorf HM (1989) Bioaccumulation and effects of selenium in wildlife. In Jacobs LM (ed) *Selenium in agriculture and the environment*. Am S Agron S Sci. Madison, Wisconsin, series number 23, pp 133–177
- Öncel MS, Muhcu A, Demirbas E, Koby M (2013) A comparative study of chemical precipitation and electrocoagulation for treatment of coal acid drainage wastewater. *J Environ Chem Eng* 1:989–995
- Picard T, Cathalifaud-Feuillade G, Mazet M, Vandesteendam C (2000) Cathodic dissolution in the electrocoagulation process using aluminum electrodes. *J Environ Monit* 2:77–80
- Presser TS, Luoma SN (2006) Forecasting selenium discharges to the San Francisco Bay-Delta Estuary: ecological effects of a proposed San Luis Drain extension. U.S. Geological Survey Professional Paper 1646
- Purkerson DG, Doblin MA, Bollens SM, Luoma SN, Cutter GA (2003) Bioavailability of particle-associated selenium on the bivalve *Potamocorbula amurensis*. *Environ Sci Technol* 34:4504–4510
- Simmons DB, Wallschlaeger D (2005) A critical review of the biogeochemistry and ecotoxicology of selenium in lotic and lentic environments. *Environ Toxicol Chem* 24:1331–1343
- Staicu LC, van Hullebusch ED, Oturan MA, Ackerson CJ, Lens PNL (2014a) Removal of colloidal biogenic selenium from wastewater (submitted to *Chemosphere*)
- Staicu LC, Ackerson CJ, Cornelis P, Ye L, Berendsen R, Hunter WJ, Noblitt SD, Henry CS, Cappa JJ, Monteneri R, Wong AO, Musilova L, Novakova M, Lens PNL, Pilon-Smits EAH (2014b) High-speed selenium oxyanion reduction by *Pseudomonas moraviensis stanleyae*, an endophyte of selenium hyperaccumulator *Stanleya pinnata* (submitted to *Syst Appl Microbiol*)
- Trompette JL, Vergnes V, Coufort C (2008) Enhanced electrocoagulation efficiency of lyophobic colloids in the presence of ammonium electrolytes. *Colloid Surface A* 315:66–73
- Turchiuli C, Fargues C (2004) Influence of structural properties of alum and ferric flocs on sludge dewaterability. *Chem Eng J* 103(1–3):123–131
- Un UT, Koparal AS, Ogutveren UB (2009) Hybrid processes for the treatment of cattle-slaughterhouse wastewater using Al and Fe electrodes. *J Hazard Mater* 164:580–586
- US EPA (2010) North San Francisco Bay selenium characterization study plan (2010–2012). <http://www2.epa.gov/sites/production/files/documents/epa-r09-ow-2010-0976-0023-1.pdf>
- US EPA Test Methods for Evaluating Solid Waste, Physical/Chemical Methods, SW-846, Method 1311. <http://www.epa.gov/osw/hazard/testmethods/sw846/pdfs/1311.pdf>
- US EPA Test Methods for Evaluating Solid Waste, Physical/Chemical Methods, SW-846, Method 1311, Chapter 7 – Characteristics, introduction and regulatory definitions. <http://www.epa.gov/wastes/hazard/testmethods/sw846/pdfs/chap7.pdf>
- USEPA (1999) Enhanced coagulation and enhanced precipitative softening guidance manual. EPA 815-R-99-012
- Vasudevan S, Oturan MA (2014) Electrochemistry: as cause and cure in water pollution—an overview. *Environ Chem Lett* 12:97–108
- Vasudevan S, Lakshmi J, Sozhan G (2009) Studies on the removal of iron from drinking water by electrocoagulation—a clean process. *Clean* 37:45–51
- Zhang Y, Zahir ZA, Frankenberger WT Jr (2004) Fate of colloidal-particulate elemental selenium in aquatic systems. *J Environ Qual* 33:559–564
- Zhu B, Clifford DA, Chellam S (2006) Comparison of electrocoagulation and chemical coagulation pretreatment for enhanced virus removal using microfiltration membranes. *Water Res* 13:3098–3108